

---

# Formal Explanations for Neuro-Symbolic AI

---

Sushmita Paul Jinqiang Yu Jip J. Dekker Alexey Ignatiev Peter J. Stuckey

Department of Data Science and AI, Faculty of IT  
Monash University, Melbourne, Victoria, Australia

{sushmita.paul,jinqiang.yu,jip.dekker,alexey.ignatiev,peter.stuckey}@monash.edu

## Abstract

Despite the practical success of Artificial Intelligence (AI), current neural AI algorithms face two significant issues. First, the decisions made by neural architectures are often prone to bias and brittleness. Second, when a chain of reasoning is required, neural systems often perform poorly. Neuro-symbolic artificial intelligence is a promising approach that tackles these (and other) weaknesses by combining the power of neural perception and symbolic reasoning. Meanwhile, the success of AI has made it critical to understand its behaviour, leading to the development of explainable artificial intelligence (XAI). While neuro-symbolic AI systems have important advantages over purely neural AI, we still need to explain their actions, which are obscured by the interactions of the neural and symbolic components. To address the issue, this paper proposes a formal approach to explaining the decisions of neuro-symbolic systems. The approach hinges on the use of formal abductive explanations and on solving the neuro-symbolic explainability problem hierarchically. Namely, it first computes a formal explanation for the symbolic component of the system, which serves to identify a subset of the individual parts of neural information that needs to be explained. This is followed by explaining only those individual neural inputs, independently of each other, which facilitates succinctness of hierarchical formal explanations and helps to increase the overall performance of the approach. Experimental results for a few complex reasoning tasks demonstrate practical efficiency of the proposed approach, in comparison to purely neural systems, from the perspective of explanation size, explanation time, training time, model sizes, and the quality of explanations reported.

## 1 Introduction

Neural Artificial Intelligence (AI) models are widely used by the decision-making procedures of many real-world applications. Their success guarantees AI will prevail as a generic computing paradigm for the foreseeable future, including in safety- and privacy-critical domains. Unfortunately, neural AI models may occasionally fail [14, 16, 60], their decisions may be prone to bias [52] or be confusing due to brittleness [19, 59], where very similar cases are treated completely differently. As a result, there is a need to understand the behaviour of AI models, analyse their potential failures, debug them, and possibly repair them. This has given rise to AI model verification [4, 33, 49, 57] and explainable AI (XAI) [38, 44, 47].

Many XAI approaches exist, including the computation of interpretable AI models [7, 34, 46] and post-hoc explanation extraction for black-box AI models [39, 53, 54]. An important approach to XAI – *formal explainable AI* (FXAI) – builds on the use of formal reasoning about the AI models of interest and on computing explanations that capture the semantics of the target models to answer “*why*” or “*why not*” they make certain decisions [27, 43, 58].

Neuro-symbolic AI is a promising paradigm developed to add symbolic reasoning to neural AI systems [3, 6, 35, 40, 45] by combining neural components (e.g., for sensory understanding) with

symbolic ones (e.g., for reasoning about sensory results). Neuro-symbolic AI systems can significantly outperform both purely neural and purely symbolic systems – as shown in several practical domains [3, 35, 40] – by taking advantage of the strengths of the two approaches, and are deemed vital for constructing rich computational cognitive models [18, 41, 62]. However, since their neural component is still an opaque black-box, the resulting decisions can still be hard or impossible for humans to comprehend. Moreover, interactions between the neural and symbolic components of the system exacerbate these problems, further deteriorating human understanding of the system’s operation.

This paper addresses these challenges by building on FXAI [43] to propose the first formal approach to the explainability of modern neuro-symbolic systems. In doing so, it considers the extraction of abductive explanations from neuro-symbolic systems where neural perception inputs are passed to the symbolic reasoner, independently of each other. The problem is tackled hierarchically, that is, given a decision made by a complex neuro-symbolic system, we start by explaining the decision of the latest component of the system and identify a subset of its inputs (passed through by the earlier components) responsible for the decision. The approach then proceeds by explaining why the latest component received these particular inputs, going backwards through the neuro-symbolic interaction. Our experimental results on a range of problem families demonstrate the usefulness and practicality of the proposed approach and its advantage over the baseline (purely neural) approach in terms of explanation size and quality. This in turn serves as an additional motivation for the development of next-generation neuro-symbolic AI.

The paper is organized as follows. [Section 2](#) overviews the background information and introduces the required concepts. [Section 3](#) discusses the proposed approach followed by the experimental results in [Section 4](#). [Section 5](#) briefly outlines related work and [Section 6](#) concludes the paper.

## 2 Preliminaries

**Datalog, Satisfiability and Unsatisfiability.** Datalog is a declarative language defined as a subset of the logic programming language Prolog, with a focus on data manipulation and querying [1]. In particular, its limited features enable the use of bottom-up evaluation, rather than the top-down evaluation common in Prolog. This makes it well-suited as a query language for deductive databases, where it can infer new facts based on existing data and rules. Answer Set Programming (ASP) languages [31] extend Datalog to include constraints and use propositional satisfiability (SAT) solving methods.

We assume standard definitions for SAT and maximum satisfiability (MaxSAT) solving [11]. A propositional formula is said to be in *conjunctive normal form* (CNF) if it is a conjunction of clauses, where a *clause* is a disjunction of literals, and a *literal* is either a Boolean variable or its negation. Whenever convenient, clauses are treated as sets of literals while CNF formulas are treated as sets of clauses. A *truth assignment* maps each variable of a formula to a value from  $\{0, 1\}$ . Given a truth assignment, a clause is said to be *satisfied* if at least one of its literals is assigned value 1; otherwise, it is *falsified* by the assignment. A formula  $\phi$  is satisfied if all its clauses are satisfied; otherwise, it is falsified. If there exists no assignment that satisfies  $\phi$ , then it is *unsatisfiable*, written  $\phi \models \perp$ .

In the context of unsatisfiable formulas, the problems of maximum satisfiability and minimum unsatisfiability are of particular interest. Hereinafter, we consider *partial* unsatisfiable CNF formulas  $\phi$  represented as a conjunction of *hard* clauses  $\mathcal{H}$ , which must be satisfied, and *soft* clauses  $\mathcal{S}$ , which are preferred to be satisfied, i.e.,  $\phi = \mathcal{H} \wedge \mathcal{S}$  (or  $\phi = \mathcal{H} \cup \mathcal{S}$  in the set theory notation). In the analysis of unsatisfiability of formula  $\phi$ , one is interested in identifying minimal unsatisfiable subsets (MUSes) of  $\phi$ , which can be defined as follows. Let  $\phi = \mathcal{H} \cup \mathcal{S}$  be unsatisfiable, i.e.,  $\phi \models \perp$ . A subset of clauses  $\mu \subseteq \mathcal{S}$  is a *Minimal Unsatisfiable Subset* (MUS) iff  $\mathcal{H} \cup \mu \models \perp$  and  $\forall \mu' \subsetneq \mu$  it holds that  $\mathcal{H} \cup \mu' \not\models \perp$ . Informally, an MUS can be seen as a minimal explanation of unsatisfiability for an unsatisfiable formula  $\phi$ . It provides the minimal information that needs to be added to the hard clauses  $\mathcal{H}$  to obtain unsatisfiability. MUS extraction is applied in our work as the underlying technology for computing formal explanations for symbolic and neural AI systems.

**Classification Problems** classify data instances into classes  $\mathcal{K}$  where  $|\mathcal{K}| = k \geq 2$ . Given a set of  $m$  features  $\mathcal{F}$ , where the value of feature  $i \in \mathcal{F}$  comes from a domain  $\mathbb{D}_i$  which may be Boolean, (bounded) integer or (bounded) real, the *complete feature space* is defined by  $\mathbb{F} \triangleq \prod_{i=1}^m \mathbb{D}_i$ . A *data point* in feature space is denoted  $\mathbf{v} = (v_1, \dots, v_m)$  where  $v_i \in \mathbb{D}_i, 1 \leq i \leq m$ . An *instance*

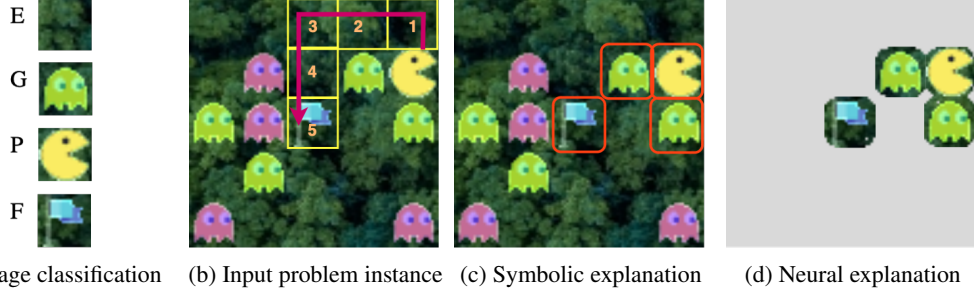


Figure 1: Example of a Pacman related puzzle aiming to find a shortest grid path from the actor’s location to the target flag. Given an input instance, the model predicts the length of a shortest path.

of a classification problem is a pair formed by a data point and its corresponding class, i.e.,  $(\mathbf{v}, c)$ , where  $\mathbf{v} \in \mathbb{F}$  and  $c \in \mathcal{K}$ . We use  $\mathbf{x} = (x_1, \dots, x_m)$  to denote an arbitrary point in feature space, where each  $x_i$  will take a value from  $\mathbb{D}_i$ . A *classifier* is a total function from feature space to class:  $\kappa : \mathbb{F} \rightarrow \mathcal{K}$ . Many approaches exist to define classifiers including decision sets [13, 34], decision lists [55], decision trees [25], random forests [17], boosted trees [12], and neural nets [24, 48].

**Example 1** Consider a simple classification function that takes a  $20 \times 20$  RGB image  $\mathbf{x} \in \mathbb{F}$  (original data are taken from [35]) and decides if it represents an empty cell  $E$ , a ghost  $G$ , an actor  $P$ , or a flag  $F$ . Example images are shown in Figure 1a. We can train a neural net classifier  $\kappa : \mathbb{F} \rightarrow \{E, G, P, F\}$  to be very accurate.  $\square$

**Neuro-Symbolic AI** is an important paradigm that bridges the gap between neural systems and logic and reasoning systems [3, 6, 35, 40, 45]. It combines the strengths of both symbolic and subsymbolic approaches by integrating logical reasoning with the powerful capabilities of deep learning. This allows neuro-symbolic models to leverage explicit domain knowledge and data-driven insights, leading to more accurate and efficient solutions for challenging AI tasks [18, 41, 62]. Scallop [35] is neuro-symbolic framework that integrates symbolic reasoning capabilities, exposed through its extended Datalog language, with the power of deep learning provided by PyTorch [9]. Through its support for differentiable programming, Scallop can seamlessly use tensors of neural networks as input or output for a symbolic program. Conversely, the same capabilities allow the back-propagation for the neural networks through a Scallop program using predefined probabilistic semantics of *provenance semirings* [20].

**Example 2** Consider a Pacman related puzzle with the task to find the length of the shortest grid path from the actor’s start location to a target flag while avoiding ghosts. The input to the puzzle shown in Figure 1b is an image consisting of  $5 \times 5$  grid cells with background and icons of either actor, target, or ghosts imposed on top. The input is a  $100 \times 100$  RGB image, and the output is the length of the shortest path from the unique actor location to the unique flag location avoiding entering any ghost location. Observe how Figure 1b also depicts a shortest path, shown in red.  $\square$

**Formal Explainability and Adversarial Robustness.** Given data point  $\mathbf{v}$  and classifier  $\kappa$ , which classifies it as class  $\kappa(\mathbf{v})$ , a *post-hoc explanation* tries to explain the behaviour of  $\kappa$  on  $\mathbf{v}$ . An *abductive explanation* (AXp) is a minimal set of features  $\mathcal{X}$  such that any data point sharing the same feature values with  $\mathbf{v}$  on these features is guaranteed to be assigned the same class  $c = \kappa(\mathbf{v})$  [27, 58]. Formally,  $\mathcal{X}$  is a subset-minimal set of features such that:

$$\forall(\mathbf{x} \in \mathbb{F}). \left[ \bigwedge_{i \in \mathcal{X}} (x_i = v_i) \right] \rightarrow (\kappa(\mathbf{x}) = c) \quad (1)$$

It is known [30, 43] that formal AXps for ML predictions are related with the concept of MUSes (defined earlier) of an *unsatisfiable* formula encoding the ML classification process  $\kappa(\mathbf{v}) = c$ , namely if one represents  $[\kappa(\mathbf{x}) \neq c]$  as hard clauses and  $[\bigwedge_{i=1}^m (x_i = v_i)]$  as soft clauses.

By examining (1), one can observe that AXps are designed to hold globally, i.e., in the entire feature space  $\mathbb{F}$ . Recent work proposed to use the tools developed for checking adversarial robustness of neural networks in the context of computing *distance-restricted* abductive explanations [23, 63].

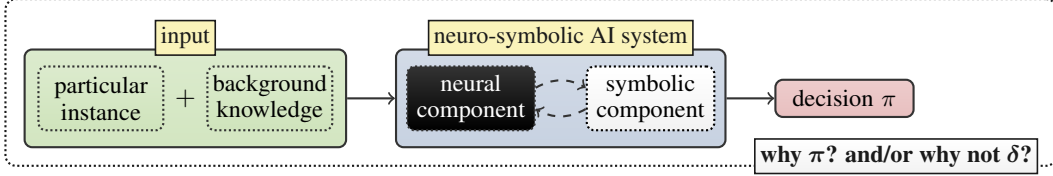


Figure 2: A general setup for explaining neuro-symbolic AI.

Namely, instead of requiring the explanation  $\mathcal{X}$  to hold for all the points  $\mathbf{x} \in \mathbb{F}$  s.t.  $\bigwedge_{i \in \mathcal{X}} (x_i = v_i)$ , we can enforce it for all compatible points in the  $\varepsilon$ -vicinity of the instance  $\mathbf{v}$  of interest:

$$\forall (\mathbf{x} \in \mathbb{F}). \left[ \bigwedge_{i \in \mathcal{X}} (x_i = v_i) \wedge \|\mathbf{x} - \mathbf{v}\|_p \leq \varepsilon \right] \rightarrow (\kappa(\mathbf{x}) = c) \quad (2)$$

where the  $\varepsilon$ -neighbourhood, s.t.  $\varepsilon \in [0, 1]$ , is defined given some  $p$ -norm,  $p \in \{0, 1, \dots, \infty\}$  [21, 56]. When  $\varepsilon = 1$ , predicate (2) equates with (1). When formally explaining a neural model, this work makes use of an adversarial robustness checker [33, 63] to decide (2), with  $\varepsilon \in (0, 1]$ .

**Example 3** Consider the Pacman shortest path example in Figure 1. Given a  $5 \times 5$  grid map with cells either empty, actor, flag or ghost, it is relatively easy to compute the shortest path symbolically, although it may be challenging for a neural agent. Explaining why the shortest path is at least some length is a bit more complex, but not difficult. Here is an informal thought process applicable in this case. The shortest path always relies on the position of the actor and the flag (if they were closer to each other, this would make the path shorter). Then for determining the ghosts relevant for the shortest path, we can remove ghosts one by one: if the shortest path does not decrease in length, then the ghost we removed is not needed to explain the shortest path. Once we have considered all ghosts, we have a minimal explanation of the shortest path. Figure 1c depicts the grid cells required to explain why the shortest path is at least distance 5 as shown in Figure 1b.  $\square$

### 3 Hierarchical Explanations

Unlike purely neural AI systems, neuro-symbolic systems are meant to delegate some responsibilities to their symbolic components. This can negatively affect the model’s interpretability. First, while purely neural models are deemed an opaque black-box whose decisions are hard for a human-decision maker to comprehend, the problem is aggravated by the (complex) interactions between the neural and symbolic components of a neuro-symbolic system. Second, such interactions arguably represent a challenge for post-hoc explanation approaches. This applies to heuristic explainers, as they are known to be susceptible to unsoundness issues [22, 42], and to formal explanation approaches, as their need to deal with many (typically NP-)hard computational problems often makes them become exponentially harder with the increase of problem complexity. The general setup for explaining a neuro-symbolic system can be seen in Figure 2.

Interestingly, the formal explainability of such hybrid neuro-symbolic systems should in fact significantly benefit from this separation of responsibilities. First, explainability of the symbolic components is naturally achievable by means of the advanced apparatus used by automated reasoning and discrete optimization for dealing with over-constrained systems [10, 29, 36, 37, 51]. Namely, the symbolic rules can be seen as a set of constraints and, given the inputs to the constraints passed by the neural component, one can use the unsatisfiability of the constraints to identify an irreducible subset of the inputs responsible for the symbolic decision. As a result, one can solve this problem by applying mechanisms similar to computing a (smallest) MUS of the set of rules, which are well understood in discrete optimization [11, Ch. 21].

Second, the functionality separation in neuro-symbolic AI leads to the simplification of the neural component as it has to deal with smaller or more focused sub-tasks, without a loss of performance of the entire neuro-symbolic system. For instance, in the Pacman setting of Figure 1, the neural component serves to provide sensor information classifying all the grid cells *individually*. This in turn may lead to structurally simpler neural models and positively impacts the performance of formal reasoning engines on such models. (Recall that scalability of formal explainability methods is often seen as one of their limitations [43].)

The above two arguments provide us with the ground for the following hierarchical approach to formal explanations for neuro-symbolic systems. Assume that we have a neuro-symbolic system whose setup implements the pipeline of Figure 2, i.e., a neural model is trained to provide sensor data to the symbolic reasoner that makes the final decision. (Note that such a setup is offered by DeepProbLog [40], Scallop [35], and Pylon [3].) In this scenario, assuming there are  $n \in \mathbb{N}$  individual inputs  $\bar{\mathbf{x}} = (\mathbf{x}_1, \dots, \mathbf{x}_n)$ ,  $\mathbf{x}_i \in \mathbb{F}$ , given to the system and, hence, the symbolic component receives  $n$  individual (and independent of each other) neural decisions coming from the neural component, the overall classification can be seen as applying a composition of functions  $c = \kappa_\sigma(\kappa_\eta(\mathbf{x}_1), \dots, \kappa_\eta(\mathbf{x}_n))$  such that the neural component computes the function  $\kappa_\eta : \mathbb{F} \rightarrow \mathbb{Y}$  and its symbolic counterpart implements  $\kappa_\sigma : \prod_{j \in [n]} \mathbb{Y} \rightarrow \mathcal{K}$ . Given a problem instance solved by such a system, an adaptation of the concept of abductive explanation answering why a neuro-symbolic system makes a certain decision can be obtained hierarchically by *going backward*. First, the hierarchical explainer extracts an abductive explanation for the symbolic decision  $c \in \mathcal{K}$ , which is provided as a subset  $\mathcal{Y} \subseteq \{1, \dots, n\}$ . Then a formal abductive explanation [43] is extracted for each of the inputs  $\mathbf{x}_j \in \mathbb{F}$ ,  $j \in \mathcal{Y}$ , independently of other inputs. Formally, hierarchical abductive explanations can be defined as follows.

**Definition 1 (Hierarchical Abductive Explanation)** *Let  $c = \kappa_\sigma(\kappa_\eta(\mathbf{x}_1), \dots, \kappa_\eta(\mathbf{x}_n))$ ,  $\mathbf{x}_j \in \mathbb{F}$ ,  $j \in [n]$ , be a decision made by a neuro-symbolic system involving a neural component  $\kappa_\eta : \mathbb{F} \rightarrow \mathbb{Y}$  and a symbolic component  $\kappa_\sigma : \prod_{j \in [n]} \mathbb{Y} \rightarrow \mathcal{K}$ . Then a hierarchical abductive explanation for decision  $c$  is a set  $\mathcal{X} = \bigcup_{j \in \mathcal{Y}} \mathcal{X}_j$  such that  $\mathcal{Y} \subseteq \{1, \dots, n\}$  is an abductive explanation for the symbolic decision  $c = \kappa_\sigma(y_1, \dots, y_n)$  and each  $\mathcal{X}_j$ ,  $j \in \mathcal{Y}$ , is an abductive explanation for the neural decision  $y_j = \kappa_\eta(\mathbf{x}_j)$ .*

A concrete example of symbolic reasoning that can be used in the case of the Pacman puzzle is provided in Example 3. In general, this can be efficiently done using a formal reasoner capable of handling the rules describing the symbolic component. For example, one can use a generic explainer for ASP programs [5] or implement a bespoke explanation extractor following the ideas behind MUS extraction widely used in the analysis of over-constrained systems (see above). (In our work, we encode the Datalog programs of Scallop into SAT and apply an efficient smallest MUS extractor [29].) The result of this step is an irreducible set of neural inputs that are deemed responsible for the symbolic decision. Next, the explainer extracts an abductive explanation for each of the individual parts of the neural inputs identified as causing the decision in the first step. Note that each such neural input is explained separately from the other inputs, by applying the methodology of formal XAI [43].

**Example 4** *Consider the problem of determining if a given handwritten binary number is greater than another binary number. Let us focus on numbers of length 3. An example of such a problem instance is depicted in Figure 3a and the prediction for this instance is false because number 0 (represented as “000”) is clearly not greater than number 5 (represented as “101”). A neuro-symbolic model can be trained with a single neural component recognizing individual bits of both numbers (separately of each other) followed by a single symbolic rule ‘ $\text{greater}(4*a + 2*b + 1*c > 4*x + 2*y + 1*z) :- d1(a), d2(b), d3(c), d4(x), d5(y), d6(z)$ ’. Here, each of the variables  $d_i(n)$  represent the corresponding predictions made by the neural component. For instance, assuming the neural component is sufficiently accurate, we can conclude that digits  $a$ ,  $b$ , and  $c$  should be predicted as 0, 0, and 0 while digits  $x$ ,  $y$ , and  $z$  are to be predicted as 1, 0, and 1. Given this information, to explain why the first number is not greater than the second, we can consider a single (pseudo-Boolean) hard constraint  $\mathcal{H} \triangleq (4a + 2b + c > 4x + 2y + z)$  and a set of soft clauses  $\mathcal{S} \triangleq \{(\bar{a}), (\bar{b}), (\bar{c}), (x), (\bar{y}), (z)\}$ . Running a smallest MUS enumerator [29] on formula  $\mathcal{H} \wedge \mathcal{S}$  results in a symbolic reason for the prediction:  $\{\bar{a}, x\}$ , shown in Figure 3b. Next, we formally explain why digits  $a$  and  $x$  are predicted by the neural component as 0 and 1, respectively, using the apparatus of FXAI, i.e., see (1) and (2). The resulting global abductive explanations are shown in Figure 3c.  $\square$*

Our hierarchical setup for computing formal abductive explanations requires all neural inputs to be independent of each other. This is motivated by the fact that *subset-minimal* hierarchical abductive explanations can be obtained by following the above approach with each of the two steps aiming for *subset-minimal* explanations  $\mathcal{Y}$  and  $\mathcal{X}_j$ ,  $\forall j \in \mathcal{Y}$ . Indeed, it is not difficult to observe that the independence of the inputs  $\mathbf{x}_j \in \mathbb{F}$  implies that we can take the union of the corresponding subset-minimal explanations  $\mathcal{X}_j$  and subset-minimality of the hierarchical explanation  $\mathcal{X}$  will be guaranteed. Formally, this can be stated as follows.



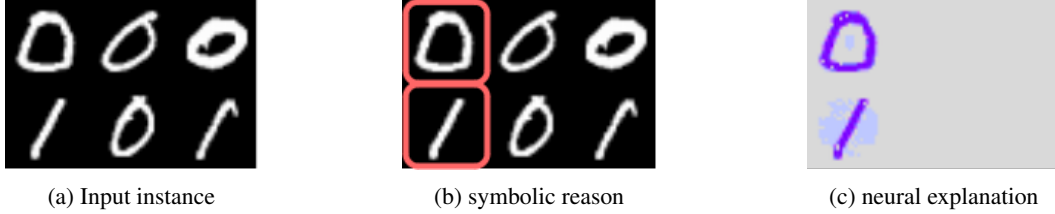


Figure 3: Hierarchical formal explanations. The system seeks to determine whether a given number handwritten in binary (top row) is greater than the other handwritten binary number (bottom row).

**Proposition 1** *Let  $c = \kappa_\sigma(\kappa_\eta(\mathbf{x}_1), \dots, \kappa_\eta(\mathbf{x}_n))$ ,  $\mathbf{x}_j \in \mathbb{F}$ ,  $j \in [n]$ , be a decision made by a neuro-symbolic system involving a neural component  $\kappa_\eta : \mathbb{F} \rightarrow \mathbb{Y}$  and a symbolic component  $\kappa_\sigma : \prod_{j \in [n]} \mathbb{Y} \rightarrow \mathcal{K}$ . Also, let a set  $\mathcal{X} = \bigcup_{j \in \mathcal{Y}} \mathcal{X}_j$  be a hierarchical abductive explanation for decision  $c$  such that  $\mathcal{Y} \in \{1, \dots, n\}$  is an abductive explanation for the symbolic decision  $c = \kappa_\sigma(y_1, \dots, y_n)$  and each  $\mathcal{X}_j$ ,  $j \in \mathcal{Y}$ , is an abductive explanation for the neural decision  $y_j = \kappa_\eta(\mathbf{x}_j)$ . Then subset-minimality of the sets  $\mathcal{Y}$  and  $\mathcal{X}_j$  s.t.  $j \in \mathcal{Y}$  guarantees that  $\mathcal{X}$  is subset-minimal.  $\square$*

Importantly, once the first step of the hierarchical approach finishes by identifying the neural “culprits” of the decision made, one may want to opt to apply a heuristic explainer [39, 53, 54] for each (or some) of the individual neural inputs (instead of the formal explainer), depending on user’s needs. Although this will affect the formal guarantees offered by FXAI methods, such an alternative may often scale better in practice. Similarly, instead of computing globally correct abductive explanations (1), one can opt for utilizing an adversarial robustness oracle and target local distance-restricted abductive explanations with a particular distance  $\varepsilon \in (0, 1)$ . As a result, the choice of the formal explainer can be seen as a trade-off between explanation soundness guarantees and the efficiency of the overall approach. Below we compare these options for several problems considered.

## 4 Experimental Results

We use three neuro-symbolic benchmarks to evaluate the scalability and quality of the explanations produced by our hierarchical explanation framework in comparison to those of pure neural approaches with similar quality prediction results. All experiments were conducted on a MacBook Pro with an Apple M3 Pro processor, with 12 CPU cores, 14 GPU cores, and 18 GB RAM. (Source code and experimental data will be made publicly available with the final version of the paper.)

### 4.1 Evaluated Explanation Methods

As our hierarchical explanation framework can flexibly combine different explanation methods for neural components, we evaluate four configurations. First, we consider the use of formal explanations for the neural components using Marabou [33] (dev. version 2024-03-11, BSD-3-Clause), a framework for verifying neural networks using SMT, and PySAT [26] (v1.8.12, MIT). Scallop is the language used to design the neuro-symbolic models (dev. version 2024-02-24, MIT). Using this method, different values of  $\varepsilon$  can be used requiring the explanation to hold for all compatible points in the  $\varepsilon$ -vicinity of the instance. We configure Marabou with  $\varepsilon = 1$ , requiring the explanation to hold for all points, in configuration HX-Marabou-e=1. The configuration HX-Marabou-e<1 uses Marabou with  $\varepsilon = 0.3$  (except for Pacman-SP where  $\varepsilon = 0.2$ ). For the third configuration HX-SHAP, we use our hierarchical framework in combination with Shapley Additive Explanations (SHAP) [39] (v0.44.1, MIT) applied for explaining the neural component. SHAP calculates the contribution of each feature to the model’s prediction for a given input, identifying the most important features. The next configuration Scallop-SHAP, directly builds (kernel) SHAP explanations for the entire neuro-symbolic model treated as a black box. The last configuration NN-SHAP uses baseline SHAP to obtain explanations for purely neural solutions for each of the given benchmarks. To achieve a similar accuracy for the purely neural applications, the size of the networks is too large for Marabou to create formal explanations within a reasonable timeframe.

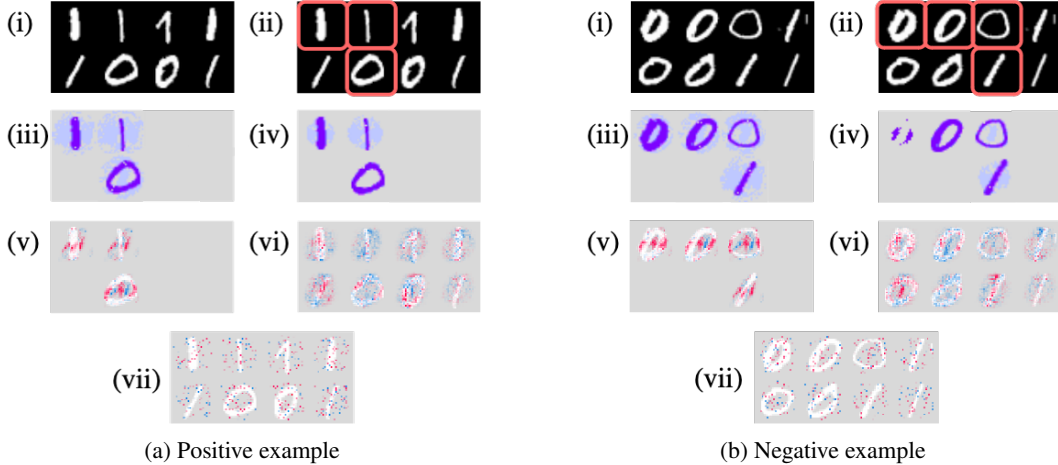


Figure 4: Given the two 4-digit binary numbers, explain whether the top number is greater than the bottom number.

## 4.2 Benchmarks and Neural Architectures

All the benchmarks are exemplified in Figures 4 to 6. In Figures 4 to 5, (i) represents the input data, (ii) the symbolic reduction, (iii) the HX-Marabou- $e=1$  explanation, (iv) the HX-Marabou- $e<1$  explanation, (v) the HX-SHAP explanation, (vi) the Scallop-SHAP explanation, and (vii) the NN-SHAP explanation. Figure 6 shows the explanations (iv)–(vii) labelled. (See Figure 1 for the other parts.)

**Lex1- $n$ .** Here we aim to learn a model that can predict the lexicographic order of two handwritten binary numbers, as discussed in Example 4 and shown in Figure 4. All tasks take as input  $n \in \{6, 8\}$  images, randomly selected from the MNIST dataset [15] filtered to only contain the digits zero and one. The combination of  $n$  images in each task is unique. The model is trained to predict whether the first number, represented by the first  $\frac{n}{2}$  images, is lexicographically greater than the second number, represented by the remaining images. In the neuro-symbolic system, a neural network predicts whether an image is zero or one, and a Scallop program then determines the lexicographic order based on the predicted values. The neural model consists of 2 fully connected hidden layers of 10 nodes. Note that the neural component is only trained indirectly through Scallop. For our pure neural application at  $n = 6$ , we employ a network that uses 2 convolutional layers, followed by 4 fully connected hidden layers with 7500, 5000, 2500, and 64 nodes sequentially. For  $n = 8$ , we use 3 convolutional layers, but use only 2 fully connected hidden layers with 1024 and 256 nodes.

**RegExp- $a$ - $n$ .** Our regular expression benchmark, an example of which is shown in Figure 5, aims to predict whether a string of 0-1 digits is in the language of regular expression  $R_a$ . Each task takes an input of  $n \in \{6, 8, 10\}$  images, randomly selected zero-one MNIST dataset similar to the Lex1- $n$  benchmark. The model is then trained to recognize whether the string represented by the images is in the language of the regular expression  $R_1 = /1.*11.*0/$ , i.e., a string starting with a one, containing two consecutive ones, and ending with a zero, or  $R_2 = /(0.*11.*)|(.*00.*1)/$ , i.e., a string that either starts with a zero and contains two consecutive ones or ends with a one and contains two consecutive zeroes. We use  $R_1$  together with the shorter string lengths  $n \in \{6, 8\}$  and  $R_2$  with  $n = 10$ . Similar to Lex1- $n$  above, the neural component predicts the digit in the images, and a Scallop program then determines whether the string is in the language of the regular expression based on the predicted values. The pure neural application for RegExp-1-6 and RegExp-2-10 have layers identical to that of the Lex1-6 benchmark, with 7500, 5000, 1024, 10 nodes in the fully connected hidden layers sequentially for both, and that of RegExp-1-8 is the same as for Lex1-8, with 1024 and 10 nodes.

**Pacman-SP.** As discussed in Examples 2 and 3 and shown in Figure 6, the aim of this benchmark is to find the length of a shortest grid path from the actor’s start position to a target flag position without stepping onto squares containing ghosts. Using the same images and obfuscation technique

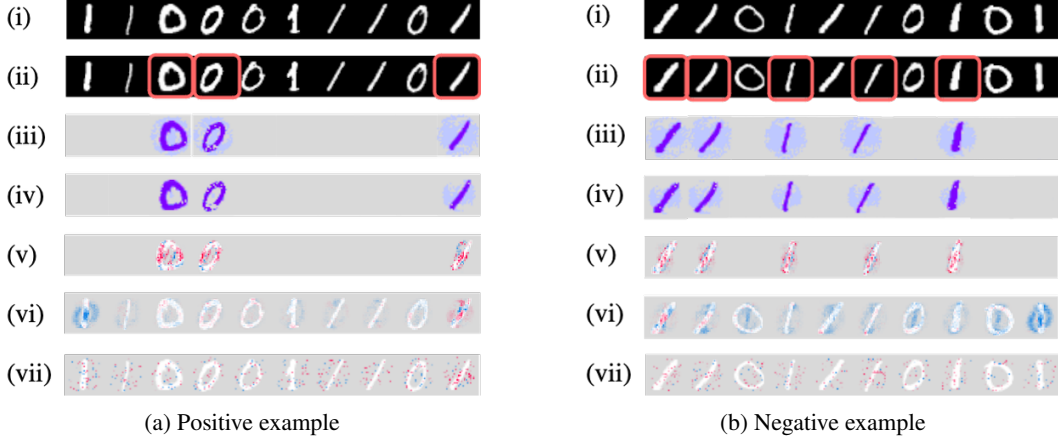


Figure 5: Explain whether the binary string is a member of the regular language  $R_2$ .

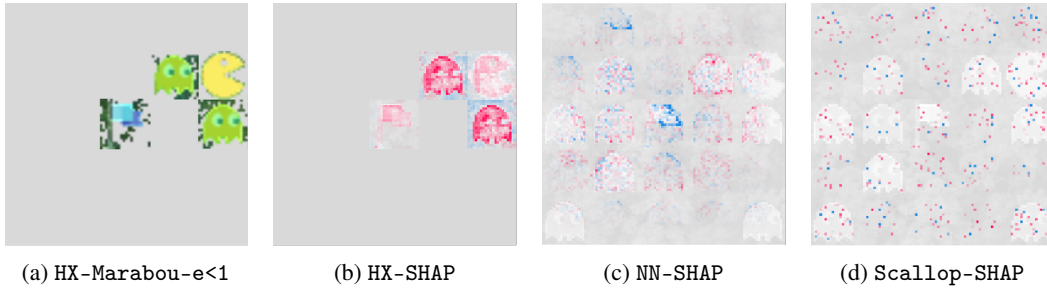


Figure 6: [extending Figure 1]. Explain why the length of the shortest path is at least 5.

as [35] (MIT), we randomly generate grids of size  $5 \times 5$  containing the actor, a target flag, and eight ghost obstacles each in a different position. Our neuro-symbolic application uses a neural network, consisting of a single fully connected layer of size 128, to predict whether a cell on the grid is empty, contains the actor, the flag, or a ghost. A Scallop program then determines the shortest path based on the predicted values. The pure neural approach uses a network with 4 convolutional layers and 3 fully connected hidden layers with 4096, 2048, and 64 nodes, respectively.

### 4.3 Evaluation

Table 1: Training time and prediction accuracy of the neuro-symbolic and purely neural models. For each model the columns depict the total training time (MM:SS), number of training epochs, time per epoch (MM:SS), final test accuracy (20% of data), and final training accuracy (80% of data).

Benchmark	Scallop (Neuro-Symbolic)					Convolutional Neural Network (CNN)				
	Time	E.	E. Time	Test (%)	Train (%)	Time	E.	E. Time	Test (%)	Train (%)
Lex1-6	00:12	3	00:04	99.90	95.00	02:42	3	00:54	98.54	96.38
Lex1-8	00:12	2	00:06	99.92	94.09	02:12	4	00:34	96.78	95.88
RegExp-1-6	00:20	5	00:04	99.50	94.45	01:43	2	00:51	99.14	98.18
RegExp-1-8	00:15	3	00:05	99.54	93.64	02:12	4	00:33	95.94	94.38
RegExp-2-10	00:24	3	00:08	99.78	94.29	05:04	3	01:41	96.70	96.54
Pacman-SP	19:36	3	06:32	100.00	99.90	31:29	12	02:37	89.15	95.98

**Model Training Time Statistics.** Table 1 shows the time required for both the Scallop and CNN models to get trained to achieve a high accuracy. In the specified number of epochs, these models obtain the mentioned accuracies for their respective benchmarks as reported in the table. Note that the epoch time in table is the time taken for training the corresponding model in a single epoch. Table 1 indicates that there is a significant training time advantage for neuro-symbolic models over CNN



models to achieve high accuracy. This is also evident as size of the architectures of the CNN models (detailed in the previous subsections) are much larger to perform the same tasks, as established in [35].

Table 2: Explanation statistics for each evaluated explanation methods and benchmarks. Columns min, avg, max, and time depict the minimum, average, and maximum explanation size, and average explanation time (MM:SS or HH:MM:SS), respectively.

Benchmark	HX-Marabou-e=1				HX-Marabou-e<1				HX-SHAP				Scallop-SHAP				NN-SHAP			
	min	avg	max	time	min	avg	max	time	min	avg	max	time	min	avg	max	time	min	avg	max	time
Lex1-6	1027	1413	2388	02:04	576	932	1648	01:54	894	1131	1790	00:01	138	430	488	08:55	2641	2687	2753	00:07
Lex1-8	733	1130	2116	02:25	302	607	1188	02:10	910	1242	2276	00:01	316	459	498	21:25	3480	3558	3612	00:04
RegExp-1-6	326	571	1854	00:50	70	328	1185	00:48	470	705	2029	00:01	233	406	492	08:31	2616	2679	2742	00:08
RegExp-1-8	496	885	2377	01:03	273	633	1866	01:26	876	1196	2190	00:01	297	435	490	16:37	3486	3550	3626	00:08
RegExp-2-10	832	1422	2778	02:42	296	742	1522	02:18	972	1570	3126	00:01	191	435	498	25:53	4408	4474	4579	00:10
Pacman-SP	721	1617	2902	08:13	398	1033	1784	10:04	800	1728	3200	00:01	391	456	522	20:45:32	6957	7038	7040	05:14

**On Explanation Sizes.** The sizes of the explanations and the average time to compute them is detailed in Table 2. The data demonstrates that the explanation size from HX-Marabou-e=1 is larger than that from HX-Marabou-e<1 (which is to be expected) and comparable to that from HX-SHAP. However, HX-Marabou-e=1 explanations are global abductive explanations and guaranteed to be correct in the entire feature space, i.e., if these input pixels are left unchanged the result will always be the same regardless of other inputs.

The average explanation sizes of HX-Marabou-e=1, HX-Marabou-e<1, HX-SHAP, Scallop-SHAP and NN-SHAP are around 16%, 9%, 18%, 7% and 60%, respectively, of the total number of features in the instance. This not only indicates that it is challenging to explain (convolutional) neural networks as large as ours but also proves the efficacy of neuro-symbolic models. Consider Figure 5a, the NN-SHAP explanations focus more on the first and last digits for the prediction, whereas common sense dictates the first digit to be irrelevant to the prediction (given the regular expression). The Scallop-SHAP explanations are also scattered around all the digits in the image, not producing any effective explanation for the prediction. Similar observations can be made w.r.t. the other examples shown, demonstrating that Scallop-SHAP and NN-SHAP essentially get lost while trying to explain the decision. Also, one can rely on explanations generated by HX-SHAP if time is a constraint, but at the cost of formal correctness.

Table 3: Percentage of neural components and explanation size for each of the evaluated explanation methods and benchmarks. Columns min, avg, and max depict percentage (%) of the minimum, average, and maximum number of neural inputs in the first row and that of explanation size in the row below, respectively.

Benchmark	HX-Marabou-e=1			HX-Marabou-e<1			HX-SHAP			Scallop-SHAP			NN-SHAP		
	min	avg	max	min	avg	max	min	avg	max	min	avg	max	min	avg	max
Lex1-6	33.33	41.83	66.67	33.33	41.83	66.67	33.33	41.83	66.67	100	100	100	100	100	100
	15.86	23.10	37.58	6.33	11.73	19.54	16.60	23.55	37.50	2.93	9.14	10.37	56.14	57.12	58.52
Lex1-8	25.00	34.12	62.50	25.00	34.12	62.50	25.00	34.12	62.5	100	100	100	100	100	100
	11.69	17.95	34.36	4.82	9.64	19.15	16.07	22.54	42.17	5.04	7.31	7.94	55.48	56.72	57.58
RegExp-1-6	16.67	23.17	66.67	16.67	23.17	66.67	16.67	23.17	66.67	100	100	100	100	100	100
	6.93	12.14	39.41	1.49	6.97	25.19	9.99	14.99	43.13	4.95	8.63	10.45	55.61	56.95	58.29
RegExp-1-8	12.50	16.75	50.00	12.50	16.75	50.00	12.50	16.75	50.00	100	100	100	100	100	100
	7.95	12.29	37.57	4.86	8.96	28.82	7.99	11.00	32.97	4.74	6.94	7.81	55.58	56.60	57.81
RegExp-2-10	20.00	30.90	60.00	20.00	30.90	60.00	20.00	30.90	60.00	100	100	100	100	100	100
	10.61	18.13	35.43	3.78	9.46	19.41	12.40	20.02	39.87	2.44	5.55	6.35	56.22	57.06	58.40
Pacman-SP	8.00	17.76	32.00	8.00	17.76	32.00	8.00	17.76	32.00	100	100	100	100	100	100
	7.21	16.17	29.02	3.98	10.33	17.84	8.00	17.28	32.00	3.91	4.56	5.22	69.57	70.38	70.40

**On Explanation Quality.** Table 3 gives insights on the percentage of features contributing to explanations. For each benchmark, the first row presents the percentage of the minimum, average and maximum number of neural inputs considered in the explanations generated through the configurations HX-Marabou-e=1, HX-Marabou-e<1, HX-SHAP, Scallop-SHAP, and NN-SHAP. The second row of

each benchmark presents the percentage of the minimum, average and maximum size of explanations, generated in all of the configurations.

Since the first three configurations follow the hierarchical symbolic reasoning, the number (and thus, the percentage) of neural inputs responsible for the explanation is same. On the contrary, explanations from the Scallop-SHAP and NN-SHAP configurations are distributed over all of the neural inputs. However, the percentage of explanation size of Scallop-SHAP, where SHAP explains the Scallop model as a blackbox, is the smallest but the explanation makes no sense. Similarly for the NN-SHAP configuration, the explanation size is nearly one-third of the total feature space, substantially losing its essence of explaining the model’s prediction. Observe that the percentage of average explanation size of HX-Marabou- $\epsilon=1$  is comparable, but lower than that of HX-SHAP (except for RegExp-1-8).

Consider the percentage of average explanation sizes for the Pacman-SP benchmark. The HX-Marabou- $\epsilon=1$  explanations that guarantees formal correctness is merely 16.17%. For the HX-Marabou configuration at  $\epsilon = 0.2$ , the percentage is 10.33. For the HX-SHAP and Scallop-SHAP configurations, the percentage is 17.28 and 4.56 respectively, and that of NN-SHAP, it is a whopping 70.38% of the entire feature space.

**Sorting Heuristics for HX-Marabou.** The quality of abductive explanations generated by HX-Marabou depends on the feature traversal procedure undertaken. Consider an image of size  $28 \times 28$  as an input, which is to be explained. If the traversal begins from the top left of the image towards the bottom right, the features on the top of the image will be eliminated first and thus, a majority of the features in an explanation will lie towards the bottom of the image. Similarly, if the traversal is initiated from the top right corner towards the bottom left, majority of the features in an explanation will lie towards the left of the image. This creates a need to apply heuristics such that our model eliminates the features that surely do not contribute to the prediction and then focusses on the important features.

In our setup, we iterate over the pixels/features based on distance from the centre of the image (of the individual neural inputs), and saturation and lightness of the pixels. The distance measure ensures that we first eliminate the features that reside close to the boundaries and the corners of the image. The saturation and lightness of pixels are considered to eliminate the darker ones first. For grayscale images of benchmarks Lex1- $n$  and RegExp- $a-n$ , the saturation and lightness measure is equivalent to the brightness of the pixel (measured by the value of the pixel: the higher, the brighter). The saturation and lightness is a reasonable measure since our benchmarks of digits and pacman grid cells have bright and/or coloured pixels that are responsible for the prediction. On applying these heuristics, the abductive explanations generated are of improved quality and give better visual representation.

## 5 Related Work

There are a large variety of approaches of XAI [38, 44, 47], including interpretable model synthesis [7, 34, 46] and post-hoc explainability of black-box ML models [39, 44, 53, 54]. The approach to explainability closest to ours is based on formal reasoning about the model of interest. It seeks to compute so-called formal abductive and contrastive explanations using a series of oracle calls to a reasoning engine and proving certain properties of the model of interest [27, 43, 58]. The area of FXAI is tightly related [28] to adversarial robustness checking and neural model verification [4, 33, 57]; hence, the reasoning engines developed in the latter community can be applied for computing formal explanations [23, 63].

Neuro-symbolic AI is often seen as a response to the weaknesses of purely neural ML architectures and often deemed crucial for constructing rich computational cognitive models where reasoning is required [6, 18, 45, 61]. A modern generation of neuro-symbolic systems implements ways to integrate conventional neural model training with the power of existing symbolic reasoning methods to solve complex problems. These systems include DeepProbLog [40], Pylon [3], and Scallop [35], which utilize Prolog, constraint modelling, and Datalog engines respectively. Due to the use of symbolic reasoning, neuro-symbolic AI is often deemed more trustable, interpretable than neural AI and also self-explanatory [2, 8, 32, 50]. We are not aware of other approaches to (formal) post-hoc explainability of neuro-symbolic AI.

## 6 Conclusions

This paper proposes a formal approach to computing abductive explanations for neuro-symbolic AI systems. The approach applies in the case of neuro-symbolic systems whose inputs are independent of each other and, as a result, implements the extraction of abductive explanations *hierarchically*. Importantly, given subset-minimal abductive explanations for the individual decisions made by the neural and symbolic components of the system, the approach is guaranteed to report a subset-minimal abductive explanation for the entire system. Experimental results obtained on a few families of benchmarks demonstrate the high quality of hierarchical explanations. A few lines of future work can be envisioned. First, it is interesting to investigate how the relaxation of the input independence requirement impacts the quality of neuro-symbolic explanations and the difficulty of their extraction. Second, while input independence facilitates our approach to the computation of subset-minimal AXps, it does not directly simplify the process of computing (i) contrastive explanations (CXps) and (ii) cardinality-minimal AXps, which we are planning to address next.

## References

- [1] Serge Abiteboul, Richard Hull, and Victor Vianu. *Foundations of Databases*. Addison-Wesley, 1995.
- [2] Andrea Agiollo and Andrea Omicini. “Measuring Trustworthiness in Neuro-Symbolic Integration”. In: *FedCSIS*. 2023, pp. 1–10.
- [3] Kareem Ahmed et al. “PYLON: A PyTorch Framework for Learning with Constraints”. In: *AAAI*. 2022, pp. 13152–13154.
- [4] Michael Akintunde et al. “Reachability Analysis for Neural Agent-Environment Systems”. In: *KR*. 2018, pp. 184–193.
- [5] Mario Alviano et al. “Explanations for Answer Set Programming”. In: *ICLP*. 2023, pp. 27–40.
- [6] Greg Anderson et al. “Neurosymbolic Reinforcement Learning with Formally Verified Exploration”. In: *NeurIPS*. 2020.
- [7] Elaine Angelino et al. “Learning Certifiably Optimal Rule Lists”. In: *KDD*. 2017, pp. 35–44.
- [8] Plamen P. Angelov et al. “Explainable artificial intelligence: an analytical review”. In: *WIREs Data Mining Knowl. Discov.* 11.5 (2021).
- [9] Jason Ansel et al. “PyTorch 2: Faster Machine Learning Through Dynamic Python Bytecode Transformation and Graph Compilation”. In: *ASPLOS (2)*. 2024, pp. 929–947.
- [10] James Bailey and Peter J. Stuckey. “Discovery of Minimal Unsatisfiable Subsets of Constraints Using Hitting Set Dualization”. In: *PADL*. 2005, pp. 174–186.
- [11] Armin Biere et al., eds. Vol. 336. *Frontiers in Artificial Intelligence and Applications*. IOS Press, 2021.
- [12] Tianqi Chen and Carlos Guestrin. “XGBoost: A Scalable Tree Boosting System”. In: *KDD*. 2016, pp. 785–794.
- [13] Peter Clark and Robin Boswell. “Rule Induction with CN2: Some Recent Improvements”. In: *EWSL*. 1991, pp. 151–163.
- [14] CNN. *Tesla Model X was in autopilot before fatal crash*. <http://tiny.cc/icjhtz>. 2018.
- [15] Li Deng. “The MNIST database of handwritten digit images for machine learning research”. In: *IEEE Signal Processing Magazine* 29.6 (2012), pp. 141–142.
- [16] Forbes. *Uber Self-Driving Car Crash: What Really Happened*. <http://tiny.cc/lcjhtz>. 2018.
- [17] Jerome H. Friedman. “Greedy Function Approximation: A Gradient Boosting Machine”. In: *The Annals of Statistics* 29.5 (2001), pp. 1189–1232.
- [18] Artur d’Avila Garcez and Luis C. Lamb. “Neurosymbolic AI: the 3rd wave”. In: *Artif. Intell. Rev.* 56.11 (2023), pp. 12387–12406.
- [19] Ian J. Goodfellow, Jonathon Shlens, and Christian Szegedy. “Explaining and Harnessing Adversarial Examples”. In: *ICLR (Poster)*. 2015.
- [20] Todd J. Green, Gregory Karvounarakis, and Val Tannen. “Provenance semirings”. In: *PODS*. 2007, pp. 31–40.
- [21] Roger A Horn and Charles R Johnson. *Matrix analysis*. Cambridge university press, 2012.

- [22] Xuanxiang Huang and João Marques-Silva. “The Inadequacy of Shapley Values for Explainability”. In: *CoRR* abs/2302.08160 (2023).
- [23] Xuanxiang Huang and Joao Marques-Silva. “From Robustness to Explainability and Back Again”. In: *CoRR* abs/2306.03048 (2023).
- [24] Itay Hubara et al. “Binarized Neural Networks”. In: *NIPS*. 2016, pp. 4107–4115.
- [25] Laurent Hyafil and Ronald L. Rivest. “Constructing Optimal Binary Decision Trees is NP-Complete”. In: *Inf. Process. Lett.* 5.1 (1976), pp. 15–17.
- [26] Alexey Ignatiev, Antonio Morgado, and Joao Marques-Silva. “PySAT: A Python Toolkit for Prototyping with SAT Oracles”. In: *SAT*. 2018, pp. 428–437.
- [27] Alexey Ignatiev, Nina Narodytska, and Joao Marques-Silva. “Abduction-Based Explanations for Machine Learning Models”. In: *AAAI*. 2019, pp. 1511–1519.
- [28] Alexey Ignatiev, Nina Narodytska, and Joao Marques-Silva. “On Relating Explanations and Adversarial Examples”. In: *NeurIPS*. 2019, pp. 15857–15867.
- [29] Alexey Ignatiev et al. “Smallest MUS Extraction with Minimal Hitting Set Dualization”. In: *CP*. 2015, pp. 173–182.
- [30] Alexey Ignatiev et al. “From Contrastive to Abductive Explanations and Back Again”. In: *AI\*IA*. 2020, pp. 335–355.
- [31] Tomi Janhunen and Ilkka Niemelä. “The Answer Set Programming Paradigm”. In: *AI Mag.* 37.3 (2016), pp. 13–24.
- [32] Subbarao Kambhampati et al. “Symbols as a Lingua Franca for Bridging Human-AI Chasm for Explainable and Advisable AI Systems”. In: *AAAI*. 2022, pp. 12262–12267.
- [33] Guy Katz et al. “The Marabou Framework for Verification and Analysis of Deep Neural Networks”. In: *CAV*. 2019, pp. 443–452.
- [34] Himabindu Lakkaraju, Stephen H. Bach, and Jure Leskovec. “Interpretable Decision Sets: A Joint Framework for Description and Prediction”. In: *KDD*. 2016, pp. 1675–1684.
- [35] Ziyang Li, Jiani Huang, and Mayur Naik. “Scallop: A Language for Neurosymbolic Programming”. In: *Proc. ACM Program. Lang.* 7.PLDI (2023), pp. 1463–1487.
- [36] Mark H. Liffiton and Ammar Malik. “Enumerating Infeasibility: Finding Multiple MUSes Quickly”. In: *CPAIOR*. 2013, pp. 160–175.
- [37] Mark H. Liffiton et al. “Fast, flexible MUS enumeration”. In: *Constraints An Int. J.* 21.2 (2016), pp. 223–250.
- [38] Zachary C. Lipton. “The mythos of model interpretability”. In: *Commun. ACM* 61.10 (2018), pp. 36–43.
- [39] Scott M. Lundberg and Su-In Lee. “A Unified Approach to Interpreting Model Predictions”. In: *NeurIPS*. 2017, pp. 4765–4774.
- [40] Robin Manhaeve et al. “Neural probabilistic logic programming in DeepProbLog”. In: *Artif. Intell.* 298 (2021), p. 103504.
- [41] Gary Marcus. “The Next Decade in AI: Four Steps Towards Robust Artificial Intelligence”. In: *CoRR* abs/2002.06177 (2020).
- [42] João Marques-Silva and Xuanxiang Huang. “Explainability Is *Not* a Game”. In: *Commun. ACM* 67.7 (2024), pp. 66–75. DOI: [10.1145/3635301](https://doi.org/10.1145/3635301). URL: <https://doi.org/10.1145/3635301>.
- [43] João Marques-Silva and Alexey Ignatiev. “Delivering Trustworthy AI through Formal XAI”. In: *AAAI*. AAAI Press, 2022, pp. 12342–12350.
- [44] Tim Miller. “Explanation in artificial intelligence: Insights from the social sciences”. In: *Artif. Intell.* 267 (2019), pp. 1–38.
- [45] Ludovico Mitchener et al. “Detect, Understand, Act: A Neuro-symbolic Hierarchical Reinforcement Learning Framework”. In: *Mach. Learn.* 111.4 (2022), pp. 1523–1549.
- [46] Christoph Molnar. *Interpretable Machine Learning*. <http://tiny.cc/6c76tz>. Leanpub, 2020.
- [47] Don Monroe. “AI, Explain Yourself”. In: *Commun. ACM* 61.11 (2018), pp. 11–13.
- [48] Vinod Nair and Geoffrey E. Hinton. “Rectified Linear Units Improve Restricted Boltzmann Machines”. In: *ICML*. 2010, pp. 807–814.
- [49] Nina Narodytska et al. “Verifying Properties of Binarized Deep Neural Networks”. In: *AAAI*. 2018.

- [50] Aritran Piplai et al. “Knowledge-Enhanced Neurosymbolic Artificial Intelligence for Cybersecurity and Privacy”. In: *IEEE Internet Comput.* 27.5 (2023), pp. 43–48.
- [51] Alessandro Previti and João Marques-Silva. “Partial MUS Enumeration”. In: *AAAI*. AAAI Press, 2013.
- [52] Julia Angwin et al. *Machine Bias*. <http://tiny.cc/dd7mjz>. 2016.
- [53] Marco Túlio Ribeiro, Sameer Singh, and Carlos Guestrin. ““Why Should I Trust You?": Explaining the Predictions of Any Classifier”. In: *KDD*. 2016, pp. 1135–1144.
- [54] Marco Túlio Ribeiro, Sameer Singh, and Carlos Guestrin. “Anchors: High-Precision Model-Agnostic Explanations”. In: *AAAI*. 2018, pp. 1527–1535.
- [55] Ronald L. Rivest. “Learning Decision Lists”. In: *Mach. Learn.* 2.3 (1987), pp. 229–246.
- [56] Derek JS Robinson. *An introduction to abstract algebra*. Walter de Gruyter, 2003.
- [57] Wenjie Ruan, Xiaowei Huang, and Marta Kwiatkowska. “Reachability Analysis of Deep Neural Networks with Provable Guarantees”. In: *IJCAI*. 2018, pp. 2651–2659.
- [58] Andy Shih, Arthur Choi, and Adnan Darwiche. “A Symbolic Approach to Explaining Bayesian Network Classifiers”. In: *IJCAI*. 2018, pp. 5103–5111.
- [59] Christian Szegedy et al. “Intriguing properties of neural networks”. In: *ICLR (Poster)*. 2014.
- [60] The Guardian. *Tesla driver killed while using autopilot was watching Harry Potter, witness says*. <http://tiny.cc/mcjhtz>. 2016.
- [61] Leslie G. Valiant. “A Theory of the Learnable”. In: *Commun. ACM* 27.11 (1984), pp. 1134–1142.
- [62] Leslie G. Valiant. “Knowledge Infusion: In Pursuit of Robustness in Artificial Intelligence”. In: *FSTTCS*. 2008, pp. 415–422.
- [63] Min Wu, Haoze Wu, and Clark W. Barrett. “VeriX: Towards Verified Explainability of Deep Neural Networks”. In: *NeurIPS*. 2023.